

# The Role of Computational Modeling in Enhancing Thermal Safety During Cardiac Ablation

Leila Seidabadi<sup>1</sup>, Indra Vandenbussche<sup>1</sup>, Rowan Carter Fink, MacKenzie Moore, Bailey McCorkendale,  
Fateme Esmailie\*

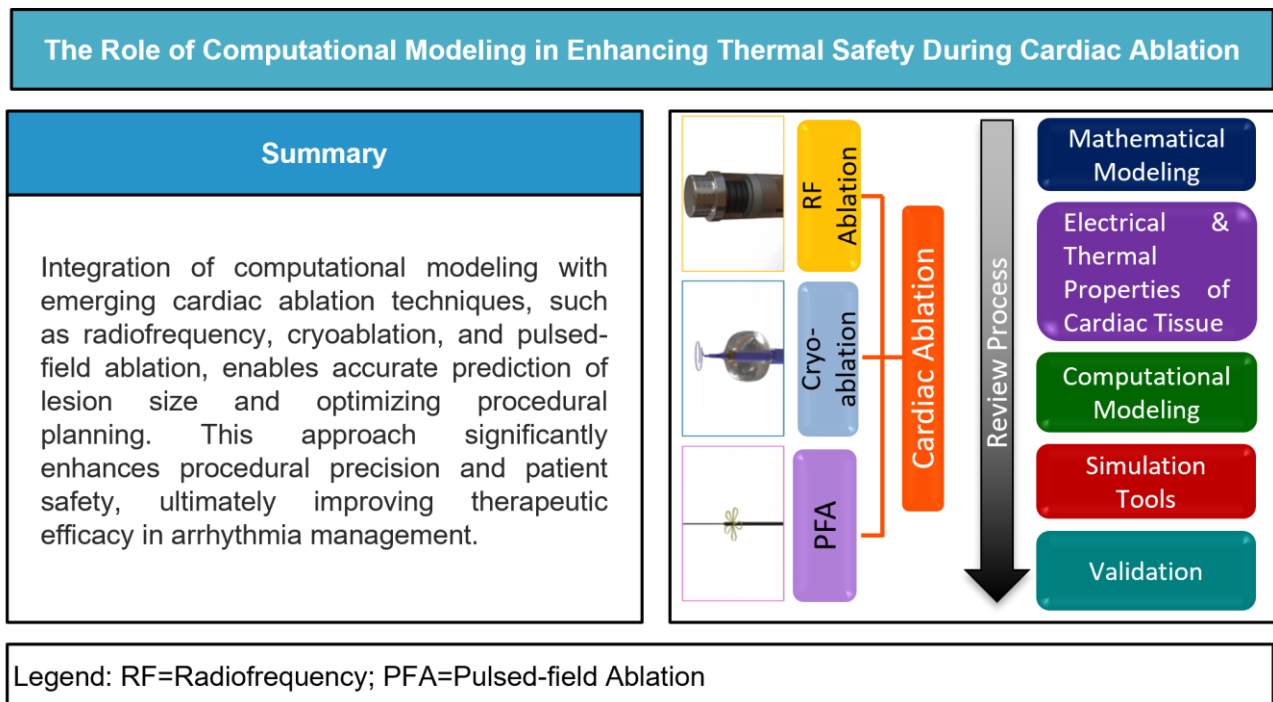
Department of Biomedical Engineering, University of North Texas, Texas, USA

\* Corresponding author. University of North Texas Discovery Park, 3940 North Elm Street, Denton, Texas 76207-7102, USA.

Tel: +1(940)3698988; E-mail: [Fateme.Esmailie@unt.edu](mailto:Fateme.Esmailie@unt.edu)

<sup>1</sup> Co-first authors

Word Count: 6365



## Abstract

**Objective:** In this review, we aim to provide an analysis of current cardiac ablation techniques, such as radiofrequency ablation (RF), cryoablation, and pulsed-field ablation (PFA), with a focus

on the role of computational modeling in enhancing the precision, safety, and effectiveness of these treatments. Particular attention is given to thermal management, exploring how computational approaches contribute to understanding and controlling energy delivery, heat distribution, and tissue response during ablation procedures.

**Methods:** The mechanisms, applications, and limitations of radiofrequency (RF) ablation, cryoablation, and pulsed field ablation (PFA) are reviewed. Additionally, the use of computational approaches, including numerical methods and artificial intelligence (AI)-based models, for evaluating energy distribution, lesion size, and tissue response during ablation procedures is discussed.

**Results:** Computational methods can predict ablation treatment outcomes and help optimize lesion size, ablation parameters, and procedural safety. However, these models are only reliable when properly validated and verified.

**Conclusion:** Further research is essential to collect reliable *in vivo* data for validating computational models and integrating them into clinical practice to improve patient outcomes.

**Keywords:** Cardiac ablation, energy distribution, lesion formation, patient-specific outcomes, computational modeling.

## ABBREVIATIONS

AF	Atrial Fibrillation
AI	Artificial Intelligence
CE	Contrast-Enhanced
CFD	Computational Fluid Dynamic
CT	Computed Tomography
DE	Delayed-Enhanced
DF	Dominant Frequency
ECG	Electrocardiogram
E-PVI	Empirical Pulmonary Vein Isolation
FDM	Finite Difference Method
FEM	Finite Element Method
FVM	Finite Volume Method
LBM	Lattice Boltzmann Method
LGE	Late Gadolinium Enhance
ML	Machine Learning
MRI	Magnetic Resonance Imaging
PFA	Pulsed-Field Ablation
PVI	Pulmonary Vein Isolation
RF	Radiofrequency
TID	Thermal Iso-effective Does
V-DF	Virtual Dominant Frequency

## 1. Introduction

The heart's conduction system is essential for effective cardiovascular function. Disruptions in the conduction system can lead to arrhythmias, which are characterized by irregular heartbeats that may manifest as tachycardia, bradycardia, or other dysrhythmias [1]. These disturbances pose significant health risks and may require treatment in the form of medication, lifestyle changes, cardioversion, or surgical interventions with cardiac ablation emerging as a key method for restoring normal sinus rhythm [2].

Cardiac ablation techniques can be categorized into several modalities, each with distinct mechanisms and applications for treating arrhythmias. Radiofrequency Ablation (RF) [3] and

Cryoablation [4] are the most widely used methods, which induce thermal damage to disrupt the arrhythmic conduction pathway [5]. RF utilizes radiofrequency waves to heat the tissue (60°C) [6], and cryoablation employs gases to achieve extremely low temperatures (below -40°C), with the gases remaining confined within the catheter and not being delivered to the tissue [7]. Pulsed Field Ablation (PFA) [8] represents a novel approach that uses high voltage pulsed electric fields to induce Irreversible Electroporation (IRE) and does not rely on thermal energy.

Alcohol ablation is used for cardiomyopathy by injecting ethanol into heart arteries; however, it carries higher hospital complication rates and uncertain long-term survival outcomes [9]. Other techniques, such as, laser ablation [10], ultrasound ablation [11], microwave ablation [12], and thermal balloon ablation [13], are rarely applied in cardiac settings due to their complexity and the expertise required (Fig. 1) [14]. Thus, these methods are not discussed in this review paper. Cryoablation, RF, and PFA, as the primary methods used in cardiac ablation, are discussed in detail (Fig. 1).

In addition to advancements in ablation techniques, the use of computational modeling to design ablation strategies and predict procedural outcomes has increased, aiming to enhance the precision and safety of cardiac ablation procedures [14]. Mathematical models and simulation tools can be used to predict temperature and electric field distribution within tissues and evaluate the extent of lesion formation, thus, enabling patient-specific treatment planning and real-time decision-making [15].

In this paper, we present an overview of current cardiac ablation techniques and their associated computational models for evaluating thermal effects.

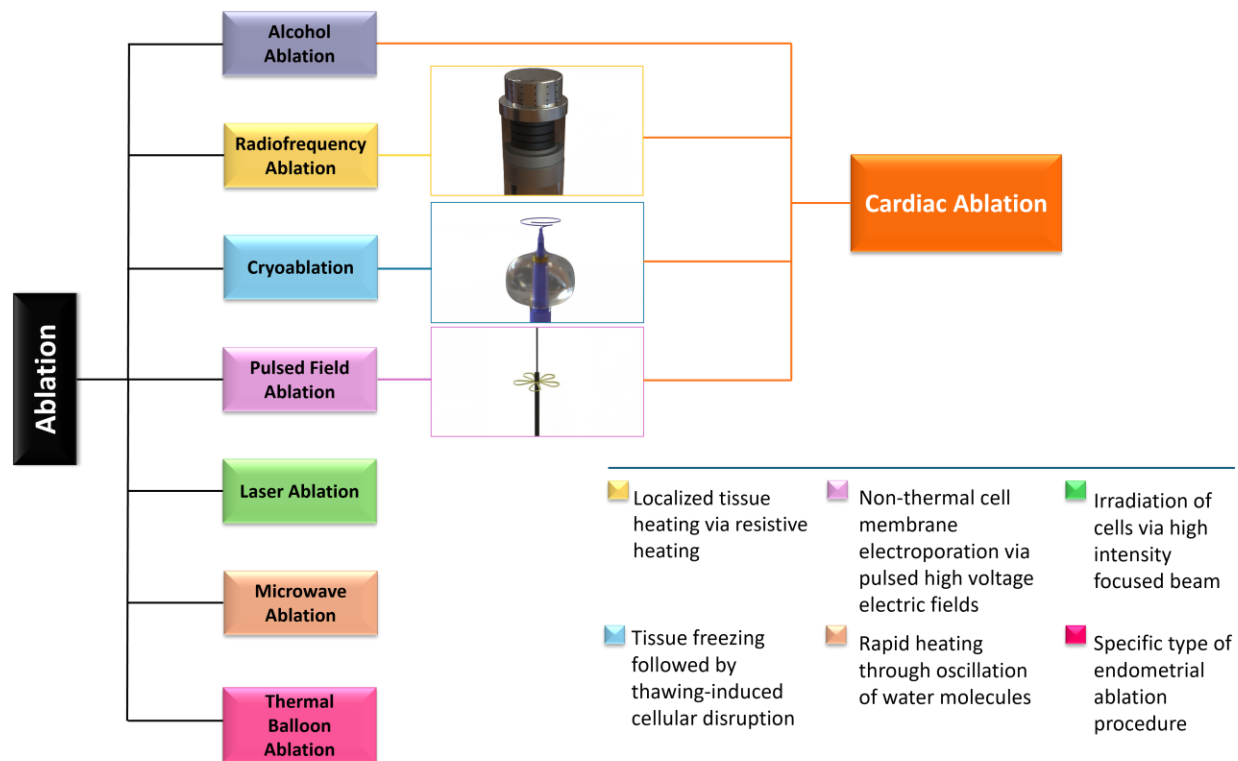


Figure 1: Schematic of ablation techniques

## 2. Overview of cardiac ablation techniques

Arrhythmias can arise from a range of physiological factors, including genetic predispositions, structural heart changes, electrolyte imbalances, and the influence of medications or stimulants [2]. In addition, pathological conditions such as ischemic heart disease, cardiomyopathy, and heart valve disorders can contribute to the development of arrhythmias [16].

Ablation techniques, particularly catheter ablation, target the areas of the heart responsible for initiating or sustaining abnormal electrical activity [17]. By precisely creating lesions to disrupt faulty electrical pathways, ablation procedures help restore normal heart rhythm, alleviate symptoms, and enhance overall cardiac function [18].

Multiple ablation techniques have been used to address different types of arrhythmias [19].

Among various cardiac ablation methods, RF ablation remains the predominant choice for cardiac

ablation, while cryoablation and PFA are utilized in more specific cases or as emerging alternatives [3]. Using RF ablation offers significant advantages, including high precision in lesion formation and proven effectiveness in maintaining sinus rhythm, particularly in atrial fibrillation patients [5]. The introduction of multielectrode irrigated catheters has further refined its application, enhanced the accuracy of lesion placement and minimized damage to surrounding tissues [20–22]. Despite RF ablation's well-recognized therapeutic benefits, it has faced several limitations, such as: 1- the risk of post-ablation thromboembolism, 2- difficulties in accessing deeper tissues, 3- unintended damage to adjacent vascular and electrical structures, and 4- challenges in evaluating electrophysiologic effects before causing irreversible local tissue damage [23]. To overcome these challenges, ablation methods utilizing alternative energy sources, such as cryoablation and PFA, have been developed to provide more effective and targeted treatment. Cryoablation procedures are associated with minimal endothelial disruption and negligible thrombus formation, enhancing their safety profile compared to traditional heat-based ablation techniques [24]. Additionally, reversible injury to cardiac tissue can be achieved when necessary, offering a unique advantage over non-reversible heat-based methods [25]. Nevertheless, reversible injury is a common limitation of cryoablation, often resulting in incomplete ablation and the need for repeat procedures to fully eliminate arrhythmogenic tissue [4]. To ensure effective treatment, sufficient cooling must be applied to achieve irreversible injury to the targeted tissue [25]. Additional risks of cryoablation include heart perforation, stroke, and damage to surrounding structures, such as the esophagus or pulmonary veins [25].

The success of RF ablation and cryoablation relies on accurate catheter placement, proper tissue contact, and controlled energy delivery. Moreover, using thermal energy can cause complications

like cardiac tamponade, thromboembolism, pulmonary vein stenosis, and damage to surrounding structures [19]. To address these limitations, PFA has emerged as a potential alternative.

PFA is an innovative technique with high-voltage, short electrical pulses that induce irreversible electroporation in targeted tissue with minimal thermal damage while preserving surrounding structures [26]. Electroporation is a physical phenomenon that occurs when tissues are exposed to high-voltage electrical energy, creating temporary or permanent nanopores in cell membranes with minimal thermal effects [27]. PFA is characterized by superior thermal safety and efficacy compared to other ablation techniques that rely on thermal energy. Thermal energy in cryoablation and RF ablation can cause prolonged tissue damage due to residual heat persisting after the energy source is deactivated [27]. The ability to generate effective lesions in a tissue-selective manner may lead to meaningful improvements in the safety of procedures, reducing complications associated with thermal ablation such as atrial-esophageal fistula and hemidiaphragmatic paralysis [28]. Moreover, the rapid nature of PFA can facilitate shorter ablation times and potentially improve patient throughput and reduce anesthesia exposure [29].

Despite PFA's advantages, this method faces several challenges that need to be addressed as technology advances. One concern is the lack of comprehensive long-term data on its safety and efficacy compared to established methods like RF ablation [30]. In addition, the absence of standardized equipment and protocols for PFA leads to variability in outcomes due to differences in energy settings and catheter designs [31].

The advantages, disadvantages, and complications of the three most common cardiac ablation methods are summarized in Table 1, highlighting the distinct benefits, risks, and effectiveness of RF ablation, cryoablation, and PFA across different patient profiles.

**Table 1. Clinical advantages and disadvantages of cardiac ablation methods**

Cardiac ablation Method	Advantages	Disadvantages
RF [123,124]	<ul style="list-style-type: none"> <li>• Lowest fluoroscopy time* [123]</li> <li>• Proven long-term efficacy in atrial fibrillation management [5]</li> <li>• Cost-effective compared to PFA or cryoablation [125]</li> <li>• Precise and controlled lesion formation [22]</li> </ul>	<ul style="list-style-type: none"> <li>• Incidences (0.016%-0.1%) of esophageal injury [124]</li> <li>• Highest risk for pulmonary vein (PV) stenosis (incidence of severe PV stenosis: 0-0.5%) [124]</li> </ul>
Cryoablation [7,25]	<ul style="list-style-type: none"> <li>• General anesthesia is not required due to the cooling effect [123]</li> <li>• Lower risk of thrombosis than RF [25]</li> <li>• Less patient discomfort [25]</li> </ul>	<ul style="list-style-type: none"> <li>• Lowest acute success [123]</li> <li>• Higher recurrent arrhythmia rate than RF [25]</li> <li>• Incidences (0.08%-0.1%) of persistent phrenic nerve (PN) palsy following pulmonary vein isolation (PVI) [124]</li> <li>• Potential reversible damage [25]</li> </ul>
PFA [19,26,27,29,126]	<ul style="list-style-type: none"> <li>• No esophageal complications, pulmonary vein stenosis, or persistent phrenic palsy [28]</li> <li>• Shortest procedure time [29]</li> </ul>	<ul style="list-style-type: none"> <li>• Coronary arterial spasm and hemolysis-related acute renal failure [28]</li> <li>• Highest total costs [31]</li> </ul>

\* Fluoroscopy involves real-time X-ray imaging during RF catheter ablation procedures [127].

The effectiveness of ablation techniques relies on balancing their benefits and limitations. Predicting potential complications before the procedure can significantly improve outcomes of cardiac ablation. Mathematical modeling is a tool that can be used to increase the success of cardiac ablation by improving preplanning, minimizing potential risks, and reducing failures, which ultimately lead to better patient outcomes.

### 3. Mathematical modeling

Mathematical modeling is essential for understanding and predicting outcomes and potential complications of cardiac ablations, such as heat-induced tissue changes and non-thermal effects,



including tissue responses and interactions with electrical fields. Mathematical models are used to improve the safety and efficacy of cardiac ablation techniques by facilitating the design of catheters, optimizing the waveforms, and reducing the potential risks [15].

Pennes bioheat transfer equation, Maxwell's equations, and the Arrhenius equation are the main equations applied to model tissue damage and the complex interactions between thermal and electromagnetic phenomena within biological tissues during cardiac ablation [32]. The subsequent sections provide a detailed discussion of these equations and their applications in cardiac ablation.

### 3.1. Bioheat transfer models

Bioheat Transfer Models, such as Pennes bioheat equation [33], the dual-phase-lag model [34], and the Weinbaum-Jiji model [35] are developed for biological tissues, accounting for metabolic heat generation and perfusion effects. Bioheat Transfer models are commonly used in medical applications such as ablation [36]. Pennes bioheat equation is the primary model used to determine heat transfer within tissues, accounting for the effects of blood perfusion and metabolic heat generation (Eq. (1)) [37]:

$$\rho c_p \frac{\partial T}{\partial t} = \nabla(k \nabla T) + \rho_b \omega_b c_{pb} (T_a - T) + Q_m + Q_{ext} \quad (1)$$

Whereas  $T$  (K) denotes the temperature of the tissue at a specified location and time,  $k$  ( $\frac{W}{m \cdot K}$ ) is the thermal conductivity of the tissue.  $\rho$  ( $\frac{kg}{m^3}$ ) and  $c_p$  ( $\frac{J}{kg \cdot K}$ ) represent the tissue density and specific heat capacity, respectively.  $\omega_b$  ( $\frac{1}{s}$ ) is the volumetric blood perfusion, accounts for

metabolic heat generation within the tissue, while  $Q_{ext} \left( \frac{W}{m^3} \right)$  represents the volumetric heat generation [38].

To derive the Pennes bioheat equation instantaneous thermal equilibrium between blood and tissue is assumed, which simplifies blood perfusion as uniform and local. Therefore, the dynamic and heterogeneous nature of vascular networks is neglected in the Pennes equation [39]. These limitations can lead to inaccuracies in predicting temperature distributions and thermal damage during ablation procedures.

Additionally, in the Pennes model, finite heat propagation speeds, thermal delays, non-Fourier heat transfer, and changes in tissue water content during overheating are overlooked. Finite heat propagation speeds and the interplay between blood flow and local tissue temperature are incorporated in the Weinbaum-Jiji and Dual-Phase-Lag models, offering a more accurate framework for predicting thermal energy distribution in biological tissues [34,35]. However, the inclusion of these terms significantly increases computational time while providing only marginal improvements in precision. Consequently, practical application of the Weinbaum-Jiji and Dual-Phase-Lag models remains limited. Despite addressing many of the Pennes bioheat equation's shortcomings, the trade-off between computational cost and accuracy makes the Pennes bioheat equation a more pragmatic and widely used choice for bioheat transfer modeling in ablation procedures [35].

Heating during RF ablation and PFA primarily results from the induction of an electromagnetic field within tissues, leading to Joule heating, potentially electrolysis, and plasma formation. Therefore, accurately modeling electromagnetic field distribution is crucial for precisely assessing

tissue damage. The current electromagnetic models applied for cardiac ablation are discussed in the next section.

### **3.2. Electromagnetic models**

Thermal modeling improves the understanding of the heat-related effects in PFA, RF ablation, and cryoablation. RF ablation and PFA techniques use electrical energy to trigger cellular effects; therefore, electromagnetic simulations are required to accurately model the interaction between electromagnetic fields and biological tissues [40]. RF ablation uses high-frequency alternating currents to cause thermal damage [41], whereas PFA employs short, high-voltage pulses to disrupt cell membranes with minimal heat [42]. Developing electromagnetic models is essential for predicting lesion size, clarifying ablation mechanisms, and optimizing procedural parameters, ultimately improving clinical outcomes and safety [43].

Electromagnetic-thermal coupled models integrate Maxwell's equations for electromagnetic fields with bioheat transfer equations to predict the spatial and temporal distribution of temperature and electric potential in the cardiac tissue surrounding the ablation zone [40]. Maxwell's equations are coupled with the Pennes bioheat equation and the Navier-Stokes equations to model the complex interactions between electromagnetic fields, heat transfer, and fluid dynamics, forming a comprehensive Multiphysics simulation [44]. Moreover, the specific absorption rate (SAR) is utilized in these simulations to quantify the heating effects generated by electromagnetic fields, ensuring accurate predictions of thermal responses and lesion formation [45]. The electromagnetic-thermal coupled models are used to determine the impact of different ablation parameters, such as discharge time [40], discharge voltage [46], and electrode size [47]

on the temperature distribution. The electric and magnetic fields distribution based on the input voltage and device geometry are included in Maxwell's equations (Eqs. (2) to (4)) [48].

$$\nabla \cdot (\sigma \nabla V) = 0 \quad (2)$$

$$E = -\nabla V \quad (3)$$

$\sigma \left( \frac{S}{m} \right)$  is the electrical conductivity of the tissue,  $V$  (V) is the electric potential, and  $E \left( \frac{V}{m} \right)$  is the electric field strength [48]. The heat source term is then given by the Joule heating equation (Eq. (4)) [49].

$$Q = \sigma |E^2| \quad (4)$$

Where  $Q \left( \frac{W}{m^3} \right)$  is the volumetric generated heat. This equation is crucial for simulating the heating patterns in RF ablation and PFA [50].

The fundamental principle of RF ablation involves generating resistive heating in cardiac tissues through the application of alternating current with frequencies between 300 kHz and 1 MHz [51]. As the current passes through the tissue, it causes water molecules near the electrode to vibrate, resulting in energy deposition, leading to thermal effects and subsequent cellular death [52]. Tissue near the electrode is heated due to the Joule heating effect, while the temperature in more distant areas primarily rises through thermal conduction and convection [53]. The volume of the lesion can be determined by considering the area that reaches temperatures above 50 °C [54]. RF ablation is governed by the Laplace equation for electric field distribution and the bioheat equation for modeling temperature changes during the procedure (Eq. (5)) [52]:

$$\nabla[\sigma(T)\nabla V] = 0 \quad (5)$$

$\sigma(T) \left( \frac{S}{m} \right)$  is the temperature-dependent electric conductivity, and  $V$  (V) is the electric potential.

Eq. (5) is incorporated a temperature-dependent conductivity term multiplied by the electric potential squared, which allows for a more accurate representation of energy absorption and temperature increase as tissue conductivity varies with temperature [55]. The temperature can be determined by solving the Pennes bioheat equation, as shown in Eq. (1) [52]. This approach enhances predictive accuracy regarding lesion formation and depth; however, it introduces computational complexity and requires precise data on tissue properties [55].

Joule heating can be included by multiplying current density by electric field intensity, offering a simpler and faster computational framework suitable for real-time applications (Eq. (6)) [56]:

$$\rho c_p \frac{\partial T}{\partial t} = \nabla(k\nabla T) + J * E - Q_h \quad (6)$$

Where  $J \left( \frac{A}{m^2} \right)$  is the current density,  $E \left( \frac{V}{m} \right)$  is the strength of the electric field, and  $Q_h \left( \frac{W}{m^3} \right)$  accounts for volumetric heat loss due to blood perfusion in the myocardial wall, which can be neglected since it is very small in comparison with other terms in Eq. (6) [57]. Crucial thermal interactions such as variable blood perfusion and velocity, two-phase water vaporization, local thermal non-equilibrium between tissue and blood phases, changes in thermal conductivity, and anisotropy of thermal properties are neglected in this model, which limits the accuracy of the thermal damage and lesion characteristics calculated using Eq. (6) [58].

PFA is distinct from traditional techniques like RF ablation, relying on high-voltage pulsed electric fields instead of alternating current [58]. Eqs. (1) and (2) are fundamental in simulating the electrical and thermal effects of PFA by modeling the electric field distribution and the energy deposition in biological tissues. Most current numerical models for predicting lesion formation during PFA are based on the principle that lesions occur when the electric field intensity exceeds

a specific threshold, known as the irreversible electroporation threshold [59]. This threshold can be affected by various factors, including the distance of the catheter from the tissue [60], pulse duration, waveform characteristics, the number of pulses delivered, and the intervals between successive pulses [61]. A quasi-static model with steady-state electric field simulation and time-dependent thermal analysis can reduce PFA modeling computational costs [62]. In this framework, it is assumed that the current density within the tissue is divergence-free, meaning there is no net accumulation or depletion of electric charge during each pulse. Mathematically, this condition is expressed as  $\nabla \cdot J = 0$ , where  $J \left( \frac{A}{m^2} \right)$  represents the current density vector. This assumption is often used in quasi-static conditions to model electric field distribution and tissue interaction during electroporation [45]. Changes in tissue electrical properties, such as conductivity and permeability, affect the electric field distribution within the system. Consequently, assuming a divergence-free field introduces inaccuracies in predicting thermal damage and electroporation-induced cell death. The mathematical models used to calculate lesion size resulting from thermal and electroporation damage are presented in Section 3.3.

### **3.3. Thermal and electroporation-induced tissue damage models**

Arrhenius equation is widely used to predict tissue thermal damage based on the cumulative effect of temperature and heating duration [63]. The Arrhenius thermal damage equation is used to calculate the probability of cell death by integrating the exposure of tissue to elevated temperatures over time [64]. A key advantage of the Arrhenius approach is its ability to model tissue damage at various temperatures, making it a flexible and powerful method in medical procedures [65]. Arrhenius's equation is expressed as follows (Eq. (7)) [64]:

$$\Omega = A \exp\left(-\frac{E_a}{RT}\right) \Delta t \quad (7)$$

Where  $\Omega$  is the thermal damage function,  $A \left(\frac{1}{s}\right)$  is the pre-exponential factor constant, a tissue-specific parameter that varies based on experimental conditions,  $E_a \left(\frac{J}{mol}\right)$  is the activation energy,  $R \left(\frac{J}{mol}\right)$  is the gas constant,  $T$  (K) is the temperature, and  $\Delta t$  (s) is the time increment. Eq. (8) is used to derive a percentage value representing cell death from thermal damage [66]:

$$ThermalDamage_{kill} = 100 * (1 - \exp(-\Omega(t))) \quad (8)$$

Another model for predicting hyperthermic injury is the Thermal Iso-effective Dose (TID) [67] or cumulative equivalent minutes at 43 (CEM<sub>43</sub>) [67–72]. The thermal equivalent minutes approach is used to determine how long a specific tissue can be maintained at a given temperature before damage occurs. Most types of tissue generally begin to experience damage at 43°C, making this temperature a critical reference point [73]. This model is commonly used to identify the heating duration required to cause thermal tissue damage and is often utilized to set safe exposure thresholds [74]. It allows non-isothermal heating conditions to be compared to isothermal heating at a reference temperature, typically set at 43°C (Eq. (9)) [69].

$$TID \text{ (or } CEM_{43}) = \int_0^t C^{(43-T(t))} dt, \quad \begin{cases} C = 0.25, & T < 43 \cdot C \\ C = 0.5, & T \geq 43 \cdot C \end{cases} \quad (9)$$

In this model,  $T(t)$  indicates the temperature applied to the target tissue at each instant,  $dt$  represents the time spent (min) at a certain temperature  $T$  (°C), and  $C$  is an adjustment factor for each 1°C change in temperature [75]. This parameter ( $C$ ) is commonly represented as  $R$  in the relevant literature. However, since we used  $R$  as the gas constant in Eq. (7), we chose an

alternative notation to avoid confusion [76]. In most soft tissues, the coagulative necrosis threshold ranges between 100 and 1000 minutes at 43°C [77].

Thermal exposure and electric field distribution are key factors in lesion formation during ablation. When the transmembrane potential surpasses a critical threshold ( $750 \left(\frac{V}{cm}\right)$  [76] -  $1000 \left(\frac{V}{cm}\right)$  [61] for  $100\mu s$  pulses), depending on the waveform configuration, irreversible electroporation causes permanent membrane disruption and cell death [78]. Understanding these dynamics is essential for analyzing lesions created by PFA ablation, as the applied electric field directly impacts the extent of cell destruction. The ratio of surviving cells after electroporation to the number of cells before treatment can be determined by Eqs. (10) to (13) [66,79]:

$$S = \frac{1}{1 + \exp\left(\frac{E - E_c(n)}{B(n)}\right)} \quad (10)$$

$$E_c(n) = E_{c0} \exp(-g_1 n) \quad (11)$$

$$B(n) = B_0 \exp(-g_2 n) \quad (12)$$

$$Electroporation_{kill} = 100 * (1 - S) \quad (13)$$

Where,  $S$  is the ratio of surviving cells after electroporation,  $E \left(\frac{V}{m}\right)$  and  $E_c(n) \left(\frac{V}{m}\right)$  denote the applied electric field and the critical electric field, respectively, which  $E_c(n)$  constitutes the critical electric field necessary for the death of 50% of the cell population.  $B(n) \left(\frac{V}{m}\right)$  is a variable that depends on the number of pulses delivered [66].  $E_0 \left(\frac{V}{m}\right)$ ,  $B_0 \left(\frac{V}{m}\right)$ ,  $g_1$ , and  $g_2$  are constant values determined through regression analysis. The regression analysis conducted utilized



electroporation properties, highlighting the scarcity of experimental data for specific tissues, including cardiac tissue [66,79,80].

Electroporation-induced and thermal cell damage, along with lesion size, are evaluated using Eqs. (7) to (13). Applying these equations does not account for the synergistic effects of thermal and electroporation-induced damage, which may lead to inaccuracies in predicting the actual survival rate [66]. In addition, Eq. (13) is derived empirically for electric pulses with microsecond durations and calibrated using data from liver tissue rather than myocardial tissue. As a result, the constants and coefficients are only valid for pulses within the microsecond range and cannot be applied to shorter or longer pulse durations. Therefore, recalibration of Eq. (13) for myocardial tissue is necessary. Other models relied on their own data set for calibration, specific to their PFA waveform and catheter geometry [61].

#### **4. Electrical and thermal properties of cardiac tissue**

Heat transfer in cardiac tissues depends on density, thermal conductivity, and specific heat capacity [81]. Myocardial tissue generally has higher thermal conductivity compared to epicardial tissue, which influences the distribution of heat during ablation procedures [81]. The effective thermal conductivity of the myocardium decreases when myocardial tissue is surrounded by fibrous and adipose tissues, and as a result, it slows down the heat transfer rate from the myocardium to the next layer of cardiac tissues [82]. Although certain models consider the dependence of properties on myocardial fiber orientation [83], the heterogeneous nature of cardiac tissue is frequently overlooked due to its inherent complexity [84].

Thermal and electrical tissue properties are determined through experimental techniques. When direct measurement is impractical, simulations and mathematical modeling serve as

complementary tools to predict the impact of these properties on final outcomes of cardiac ablation. Ex vivo measurement of thermal properties is often unreliable due to lack of perfusion [81]. Statistical information found in databases can provide valuable insights into the variability of tissue properties [85]. A list of the thermal and electrical property values incorporated in cardiac ablation computational models is presented in Table 2.

It should be noted that the properties of cardiac tissue are affected by temperature, pressure, electrical field, and the type of tissue involved [84]. For instance, an increase in temperature during cardiac ablation enhances tissue thermal conductivity, and the electrical field can alter the electrical conductivity of the tissue [86].

**Table 2. Electrical and thermophysical properties of cardiac tissues and ablation catheter**

Material	$\sigma_0 \left(\frac{S}{m}\right)$	$\sigma_1 \left(\frac{S}{m}\right)$	$k \left(\frac{W}{m \cdot K}\right)$	$\rho \left(\frac{kg}{m^3}\right)$	$c_p \left(\frac{J}{kg \cdot K}\right)$
Electrode	4.6 x10 <sup>6</sup> [86]	-	71 [86]	21,500 [86]	132 [86]
Catheter	10 <sup>-5</sup> [86]	-	23 [86]	1440 [86]	1050 [86]
Saline water	1.392 [86]	-	0.628 [86]	980 [86]	4184 [86]
Epicardial fat/ adipose tissue	0.0377 [86] 0.0684 [85]	0.0438 [86]	0.21 [85]	911 [85]	2348 [85]
Heart/ myocardium	0.0537 [86] 0.733 [85]	0.281 [86]	0.56 [85]	1081 [85]	3686 [85]
Cardiac chamber/ blood	0.7 [86] 1.23 [85]	0.748 [86]	0.52 [85]	1050 [85]	3617 [85]
Connective tissue*	0.1199 [86] 0.490 [85]	-	0.35 [86] 0.39 [85]	1000.5 [86] 1027 [85]	2884.5 [86] 2372 [85]

$\sigma$ : electrical conductivity ( $\sigma_0$  and  $\sigma_1$  are the pre- and post-electroporation conductivity values, respectively);  $k$ : thermal conductivity;  $\rho$ : density;  $c_p$ : specific heat

\*Mixture of 50% fat and 50% muscle

Once the mathematical model and thermal-electrical properties are defined, the next step in simulating the cardiac ablation procedure is selecting an appropriate computational method to

solve the governing equations and predict treatment outcomes, as discussed in the following sections.

## **5. Computational modeling approaches**

Computational modeling is essential for predicting tissue damage during ablation procedures, which helps to predict treatment outcomes and optimize treatment parameters [87]. The choice of computational method for ablation modeling depends on the complexity of the procedure, the required precision, and the available computational resources [88]. The most common computational approaches in ablation involve applying numerical methods to solve momentum, mass, and energy balance equations [89] and/or utilizing Artificial Intelligence (AI) to develop mathematical correlation models trained on existing data (Table 3) [90,91].

The interaction between tissue, ablation catheter, and blood flow during ablation may significantly impact heat dissipation and lesion formation, potentially altering the depth and size of the lesions [92]. During atrial fibrillation ablation procedures, computational fluid dynamics (CFD) method is particularly valuable for modeling blood flow within the heart's chambers and evaluating the cooling effects of blood flow to ensure effective lesion formation [93].

In addition, development of patient-specific models is facilitated by recent advancements in computational methods, enabling individualized treatment planning for both atrial and ventricular ablation procedures [94].

Several numerical methods are used in ablation modeling, each suited to specific scenarios. Finite Element Method (FEM) is widely used because it can provide detailed simulations, though it can be computationally expensive for large-scale or transient simulations [95]. FEM is utilized to

simulate thermal and mechanical responses during ablation and is commonly applied for its flexibility in handling complex geometries and boundary conditions, especially in RF ablation [96]. The Finite Difference Method (FDM) is simpler to implement and requires fewer computational resources, but it has limitations with complex geometries and provides less accurate results. FDM can be applied effectively for one- or two-dimensional problems, such as thermal diffusion along a linear catheter path [97].

The Finite Volume Method (FVM) is another numerical technique for modeling ablation problems, particularly when blood flow plays a crucial role in thermal ablation scenarios. FVM is used to simulate various aspects of ablation, including the blood velocity fields and friction coefficient variations by ensuring the conservation of mass, momentum, and energy within the control volumes [98]. FVM has been applied to various ablation applications, including RF ablation and cryoablation, enabling the simulation of ablation zones, temperature distributions, and ablation efficiency [99].

The Lattice Boltzmann Method (LBM) is employed to solve the governing equations involved in complex heat-fluid interactions, such as tissue vaporization during ablation. It provides a numerical framework for fluid dynamics at the macroscopic scale, based on kinetic equations formulated at the mesoscopic scale [100]. Mono-domain cardiac electrophysiology can be efficiently simulated using LBM [101]. LBM's capacity in handling complex geometries and boundary conditions makes it ideal for modeling the detailed aspects of PFA procedures [102].

In the context of ablation, AI techniques, especially Machine Learning (ML), can be applied to optimize treatment protocols by extracting significant parameters that impact the treatment outcomes from the existing patient data [103]. AI-based models are increasingly being

incorporated into ablation modeling to optimize parameters and predict real-time outcomes. Algorithms in the ML methods are used to optimize ablation strategies (e.g., placement of probes) to achieve desired outcomes with minimal damage to healthy tissue [104]. For instance, clinicians can use ML models to process intraoperative data for monitoring and predicting ablation zone growth. The macro-classification method in ML has been applied to RF ablation [105]. ML models have been used to predict outcomes using clinical data and electrograms, offering insights into tissue damage during the freezing process [106]. Integrating electrogram and electrocardiogram signals with clinical data through ML can improve predictions of atrial fibrillation recurrence after PFA ablation [107].

In summary, FEM is the primary numerical method for accurately simulating thermal damage in RF and cryoablation, while FDM is used for fast response and simplified 1D and 2D computational models. ML methods are growing in use for predicting patient-specific outcomes and enabling personalized treatments. FVM and LBM are utilized in atrial and ventricular applications where blood flow significantly impacts ablation outcomes (Table 3). Despite advances in computational models for predicting cardiac ablation outcomes, the development and validation of multiphysics, patient-specific simulations capable of accurately predicting lesion size and tissue damage remain active areas of research, particularly for emerging techniques like PFA. A major challenge in this field is designing a computational algorithm that can simultaneously solve the Navier-Stokes, Maxwell, and Pennes equations in complex geometries. Developing such algorithms is time-intensive and requires highly skilled experts. To expedite this process, commercially available software provides user-friendly interfaces and preprogrammed solvers, reducing the

effort needed for algorithm development. The next section discusses the available software options for these simulations.

**Table 3. Computational Modeling for atrial and ventricular ablation**

Geometry	Computational modeling method	Ablation method	Ablation Pattern	Is thermal damage assessed?	Is electroporation assessed?
Atrial	FEM	RF	Phase singularity-based and Dominant Frequency (DF)-based [128]	×	×
			Focused on rotor ablation using basket catheter strategies [129]	×	×
			Focus on lesion modeling [130]	√	×
			Pulmonary Vein Isolation (PVI) [131]	×	√
		PFA	Dose-dependent lesion depth correlated with voltage and tissue contact [60]	×	√
			Focus on lesion modeling (thermal and IRE ablation effects) [89]	√	√
			PVI [132]	×	√
		Cryoablation	PVI [133]	√	×
			PVI [134]	√	×
		FDM	RF	PVI [135]	×
	DF-based ablation [136]			×	×
	Reentrant driver defined by 3D structural "fingerprints" in Atrial Fibrillation (AF) [137]			×	×
	ML	RF & Cryoablation	PVI and additional ablation lines based on clinical need [138]	×	×
			PVI [139]	×	×
			PVI [140]	×	×
Ventricular	FEM	RF	No specific ablation pattern mentioned [141]	√	×
			Substrate-based ablation for ventricular tachycardia [91]	×	×
			Focuses on computational lesion modeling [121]	√	×
		PFA	Focus on lesion modeling (optimization of IRE protocols for myocardial decellularization and damage control) [142]	√	√
			No specific ablation pattern mentioned, focused on lesion morphology [61]	√	√
		ML	RF	Substrate-based ablation [143]	×

×No      √ Yes

## **6. Computational modeling platforms for cardiac ablation simulations**

COMSOL Multiphysics is widely used for modeling ablation due to its multiphysics capabilities, enabling the integration of electromagnetic, bioheat transfer, and fluid dynamics modules [108]. Researchers use COMSOL Multiphysics to incorporate temperature-dependent properties, model multiple physics interactions simultaneously, and integrate user-defined functions [108]. COMSOL is utilized to model temperature distribution within the ablation catheter and cardiac tissues during PFA and to evaluate the effects of pulse number and electrical conductivity on cell ablation and thermal damage [66]. However, integrating multiple physics, such as electromagnetic, bioheat transfer, and fluid dynamics, significantly increases the complexity of setting up and running simulations in COMSOL, primarily due to its FEM-based approach. Thus, when blood flow plays a critical role in determining lesion size, COMSOL may not be the most suitable option.

ANSYS provides extensive tools for fluid dynamics, thermal, and electromagnetic simulation, making it a desirable tool for modeling PFA [109]. ANSYS electromagnetic module, high-frequency structure simulator (HFSS), is advantageous for high-frequency applications like RF ablation. Additionally, ANSYS transient thermal module can be used to incorporate temperature-dependent blood perfusion in thermal modeling [110]. Temperature-dependent properties can be incorporated into ANSYS models to enhance the precision of electrode design optimization and ablation parameter determination [111]. The learning curve for ANSYS is steeper than COMSOL, as COMSOL offers a highly intuitive and user-friendly interface. Additionally, performing thermal analysis and post-processing in ANSYS is more complex, requiring a highly experienced user. In complex cases, programming languages and numerical computing

environments such as MATLAB and Python are used to develop customized models, either independently or in conjunction with software like COMSOL and ANSYS.

MATLAB is utilized for modeling and simulating cardiac ablation, enabling temperature distribution control, energy delivery optimization, and lesion characterization under varying blood flow conditions [46,63]. It is also used to analyze catheter position and stability, supporting improved lesion quality and procedural outcomes [112]. Both MATLAB and COMSOL have shown high applicability in assessing tissue responses to cardiac ablation, with some studies integrating both platforms for a comprehensive approach to refining ablation strategies [113].

Python tools are utilized for creating sophisticated simulations and ML models for cardiac ablation application [114,115]. Applications such as predicting cardiac ablation outcomes and optimizing procedural strategies demonstrate Python's versatility in analyzing complex medical data and training advanced models [116].

Cardiac ablation simulations may not reflect real-life outcomes without validation and verification. Therefore, systematic verification and validation are essential to ensure the reliability of computational models. The following section discusses the validation process and recent research addressing this need.

## **7. Validation of cardiac ablation simulations**

Validation is primarily used to refine and improve a computational model to ensure it accurately represents reality. Once this is achieved, the validated model can be trusted for use in the decision-making process and clinical settings, providing reliable insights to guide treatments and procedural strategies [117]. A key focus of recent research is improving the precision and



effectiveness of cardiac ablation simulations by comparing their results with clinical outcomes in cardiac ablation [118].

Only a limited number of cardiac ablation models have been validated using experimental data. For instance, a model of irrigated RF ablation was validated by comparing temperature, lesion width, and depth between simulations and experiments [119]. In this study, for perpendicular catheter orientation, errors were 6.2°C for maximum gel temperature, 0.7 mm (10.9%) for lesion width, and 0.3 mm (7.7%) for lesion depth [119]. These errors highlight the limitations of model accuracy in predicting thermal effects during cardiac ablation. While the discrepancies prevent full confidence in the computational model, they help identify inaccuracies and guide model improvements.

Open-irrigated electrodes optimize power delivery while maintaining low temperatures. As another example, the computational model of ThermoCool (6-hole) and ThermoCool® SF (multi-hole) catheter electrodes for endocardial RF ablation were validated against experimental lesion dimensions [120]. Differences between computational model and experiment in lesion depth were below 1 mm, while lesion width varied within 1-2 mm, following 30 and 60 seconds of RF ablation at 20W and 35W [120]. Based on the validation results, the model accurately predicts lesion depth within acceptable limits, while deviations in lesion width highlight the need for further refinement to improve accuracy [120].

Lesion size depends on the power dissipated in the tissue, which is influenced by the electrode's contact area [121]. In a computational model of radiofrequency catheter ablation with open-irrigated electrodes, lesion depth was validated by comparing computational model results with *in vitro* porcine myocardium experiments, yielding errors from -1.16% to +5.42% [121]. The

model underestimated lesion width by 9–23% and predicted the maximum lesion width at a greater depth than observed experimentally, overestimating it by up to 52%. This suggests the computational model may overestimate heat penetration into deeper tissue, possibly due to assumptions regarding thermal conductivity, tissue perfusion, or energy distribution [121]. These results highlight the need for further model improvements, such as incorporating tissue structure, to enhance accuracy [121].

These examples underscore the criticality of validating and refining computational models to achieve reasonable accuracy before their application in clinical decision-making. Validation of cardiac ablation models with *in vivo* experimental data is challenging due to tissue variability, the heart's dynamic environment, and difficulties in real-time measurement. Indirect imaging methods have limitations, and ethical and logistical constraints make *in vivo* testing costly and complex [122]. *In vitro* models serve as alternative systems for collecting experimental data but lack the effects of perfusion, cardiac dynamics, and thermophysical property variations. Consequently, many studies rely on computational modeling without comprehensive validation and verification. Validation and verification of computational models are critical across engineering disciplines, with standards such as ASME V&V 20-2009 and ASME V&V 40-2018 providing guidelines for biomedical applications.

In summary, a key knowledge gap in computational cardiac ablation is the lack of experimental data for validating simulation results. Potential solutions include developing non-invasive measurement techniques, utilizing AI to extract data from current measurement modalities such as MRI, CT, ultrasound, and echocardiography, and fabricating realistic *in vitro* models using advanced organoid and tissue printing technologies.

## 8. Conclusions and future directions

A comprehensive review of computational methods used in cardiac ablation treatments is provided in this paper, offering new insights to propel future research in the field. Physics-driven models alongside emerging AI-based models are discussed in this paper. The significant potential of computational modeling to enhance the planning, execution, and prediction of outcomes in cardiac ablation procedures is highlighted in this paper.

Despite the advancements in cardiac ablation modeling, a significant challenge remains the scarcity of comprehensive *in vivo* experimental data for thorough validation. The limited availability of detailed lesion measurements in various cardiac tissues and ablation techniques hinders the refinement and validation of these models. To address this, future research should prioritize the acquisition of high-quality experimental data, including detailed lesion size, depth, and transmural measurements, across a range of ablation parameters and tissue types.

To transition computational models from experimental research to routine clinical practice, it is essential to integrate patient-specific models with lesion prediction models to enhance accuracy and clinical applicability. Patient-specific models are constructed using high-resolution intraoperative imaging and post-procedural histopathology. By incorporating patient-specific anatomical and physiological data into lesion prediction simulations, clinicians can dynamically refine ablation strategies to optimize lesion placement and minimize collateral damage.

Integrating machine learning with computational fluid-thermal-electrical models enables real-time simulation of cardiac ablation, supporting clinical decision-making and adaptive treatment strategies based on patient-specific responses. Transitioning these models from research to

routine clinical practice requires large-scale, multi-center validation studies to ensure predictive accuracy and safety.

## **FUNDING**

The authors gratefully acknowledge the support of Fields Medical, Inc. [Grant No: GFP00144], and the University of North Texas for funding this research.

**Conflict of interest:** none declared.

## **DATA AVAILABILITY**

No new data were generated or analyzed in support of this research.

## **Author contributions**

**Leila Seidabadi** and **Indra Vandenbussche:** Contributed equally to the conceptualization; Literature review; Writing-original draft; Supervision; Writing-review and editing. **Rowan Carter Fink:** Contributed to data collection, visualization; writing-original draft. **MacKenzie Moore:** Contributed to literature review; writing-review and editing. **Bailey McCorkendale:** Contributed to literature review; writing-review and editing. **Fateme Esmailie:** Contributed to supervision; conceptualization; resources; writing-review and editing. All authors read and approved the final manuscript.

## References

- [1] Karpawich PP. Pathophysiology of Cardiac Arrhythmias: Arrhythmogenesis and Types of Arrhythmias. *Pathophysiology and Pharmacotherapy of Cardiovascular Disease*, Cham: Springer International Publishing; 2015, p. 1003–14. [https://doi.org/10.1007/978-3-319-15961-4\\_47](https://doi.org/10.1007/978-3-319-15961-4_47).
- [2] Kingma J, Simard C, Drolet B. Overview of Cardiac Arrhythmias and Treatment Strategies. *Pharmaceuticals* 2023;16:844. <https://doi.org/10.3390/ph16060844>.
- [3] Wray JK, Dixon B, Przkora R. Radiofrequency Ablation. 2025.
- [4] Avitall B, Kalinski A. Cryotherapy of cardiac arrhythmia: From basic science to the bedside. *Heart Rhythm* 2015;12:2195–203. <https://doi.org/10.1016/j.hrthm.2015.05.034>.
- [5] Calkins H, Hindricks G, Cappato R, Kim Y-H, Saad EB, Aguinaga L, et al. 2017 HRS/EHRA/ECAS/APHRS/SOLAECE expert consensus statement on catheter and surgical ablation of atrial fibrillation. *Heart Rhythm* 2017;14:e275–444. <https://doi.org/10.1016/j.hrthm.2017.05.012>.
- [6] Gupta D, Al-Lamee RK, Earley MJ, Kistler P, Harris SJ, Nathan AW, et al. Cryoablation compared with radiofrequency ablation for atrioventricular nodal re-entrant tachycardia: analysis of factors contributing to acute and follow-up outcome. *EP Europace* 2006;8:1022–6. <https://doi.org/10.1093/europace/eul124>.
- [7] Erinjeri JP, Clark TWI. Cryoablation: Mechanism of Action and Devices. *Journal of Vascular and Interventional Radiology* 2010;21:S187–91. <https://doi.org/10.1016/j.jvir.2009.12.403>.
- [8] Verma A, Haines DE, Boersma L V., Sood N, Natale A, Marchlinski FE, et al. Pulsed Field Ablation for the Treatment of Atrial Fibrillation: PULSED AF Pivotal Trial. *Circulation* 2023;147:1422–32. <https://doi.org/10.1161/CIRCULATIONAHA.123.063988>.
- [9] Sorajja P, Valeti U, Nishimura RA, Ommen SR, Rihal CS, Gersh BJ, et al. Outcome of Alcohol Septal Ablation for Obstructive Hypertrophic Cardiomyopathy. *Circulation* 2008;118:131–9. <https://doi.org/10.1161/CIRCULATIONAHA.107.738740>.
- [10] Fan Y, Xu L, Liu S, Li J, Xia J, Qin X, et al. The State-of-the-Art and Perspectives of Laser Ablation for Tumor Treatment. *Cyborg and Bionic Systems* 2024;6. <https://doi.org/10.34133/cbsystems.0062>.
- [11] Zhou Y-F. High intensity focused ultrasound in clinical tumor ablation. *World J Clin Oncol* 2011;2:8. <https://doi.org/10.5306/wjco.v2.i1.8>.
- [12] Lubner MG, Brace CL, Hinshaw JL, Lee FT. Microwave Tumor Ablation: Mechanism of Action, Clinical Results, and Devices. *Journal of Vascular and Interventional Radiology* 2010;21:S192–203. <https://doi.org/10.1016/j.jvir.2010.04.007>.
- [13] Baldwin SA, Pelman A, Bert JL. A Heat Transfer Model of Thermal Balloon Endometrial Ablation. *Ann Biomed Eng* 2001;29:1009–18. <https://doi.org/10.1114/1.1415521>.

- [14] Wu Z, Liu Y, Tong L, Dong D, Deng D, Xia L. Current progress of computational modeling for guiding clinical atrial fibrillation ablation. *Journal of Zhejiang University-SCIENCE B* 2021;22:805–17. <https://doi.org/10.1631/jzus.B2000727>.
- [15] Dunne E, Baena-Montes JM, Donaghey K, Clarke C, Kraśny MJ, Amin B, et al. A Predictive and an Optimization Mathematical Model for Device Design in Cardiac Pulsed Field Ablation Using Design of Experiments. *J Cardiovasc Dev Dis* 2023;10:423. <https://doi.org/10.3390/jcdd10100423>.
- [16] Markides V. Atrial fibrillation: classification, pathophysiology, mechanisms and drug treatment. *Heart* 2003;89:939–43. <https://doi.org/10.1136/heart.89.8.939>.
- [17] Ghzally Y, Ahmed I, Gerasimon G. *Catheter Ablation*. 2025.
- [18] Kumar S, Barbhैया CR, Balindger S, John RM, Epstein LM, Koplan BA, et al. Better Lesion Creation And Assessment During Catheter Ablation. *J Atr Fibrillation* 2015;8:1189. <https://doi.org/10.4022/jafib.1189>.
- [19] McBride S, Avazzadeh S, Wheatley AM, O'Brien B, Coffey K, Elahi A, et al. Ablation Modalities for Therapeutic Intervention in Arrhythmia-Related Cardiovascular Disease: Focus on Electroporation. *J Clin Med* 2021;10:2657. <https://doi.org/10.3390/jcm10122657>.
- [20] Sebag AFWM. Cardiac electrophysiology: evolution of the technique over the last decade. *EuropeanSocietyofCardiology* 2022;21.
- [21] Joseph JP, Rajappan K. Radiofrequency ablation of cardiac arrhythmias: past, present and future. *QJM* 2012;105:303–14. <https://doi.org/10.1093/qjmed/hcr189>.
- [22] Verma A, Schmidt MM, Lalonde J-P, Ramirez DA, Getman MK. Assessing the Relationship of Applied Force and Ablation Duration on Lesion Size Using a Diamond Tip Catheter Ablation System. *Circ Arrhythm Electrophysiol* 2021;14. <https://doi.org/10.1161/CIRCEP.120.009541>.
- [23] Olson M, Nantsupawat T, Sathnur N, Roukoz H. *Cardiac Ablation Technologies*. Eng Med, Elsevier; 2019, p. 83–118. <https://doi.org/10.1016/B978-0-12-813068-1.00004-X>.
- [24] Friedman PL. Catheter Cryoablation of Cardiac Arrhythmias. *US Cardiology Review* 2004;1:126–8. <https://doi.org/10.15420/usc.2004.1.1.126>.
- [25] Andrade JG, Khairy P, Dubuc M. Catheter Cryoablation. *Circ Arrhythm Electrophysiol* 2013;6:218–27. <https://doi.org/10.1161/CIRCEP.112.973651>.
- [26] Younis A, Zilberman I, Krywaczyk A, Higuchi K, Yavin HD, Sroubek J, et al. Effect of Pulsed-Field and Radiofrequency Ablation on Heterogeneous Ventricular Scar in a Swine Model of Healed Myocardial Infarction. *Circ Arrhythm Electrophysiol* 2022;15. <https://doi.org/10.1161/CIRCEP.122.011209>.

- [27] Chun K-RJ, Miklavčič D, Vlachos K, Bordignon S, Scherr D, Jais P, et al. State-of-the-art pulsed field ablation for cardiac arrhythmias: ongoing evolution and future perspective. *Europace* 2024;26. <https://doi.org/10.1093/europace/euae134>.
- [28] Ekanem E, Neuzil P, Reichlin T, Kautzner J, van der Voort P, Jais P, et al. Safety of pulsed field ablation in more than 17,000 patients with atrial fibrillation in the MANIFEST-17K study. *Nat Med* 2024;30:2020–9. <https://doi.org/10.1038/s41591-024-03114-3>.
- [29] Iyengar SK, Iyengar S, Srivathsan K. The promise of pulsed field ablation and the challenges ahead. *Front Cardiovasc Med* 2023;10. <https://doi.org/10.3389/fcvm.2023.1235317>.
- [30] Turagam MK, Neuzil P, Schmidt B, Reichlin T, Neven K, Metzner A, et al. Safety and Effectiveness of Pulsed Field Ablation to Treat Atrial Fibrillation: One-Year Outcomes From the MANIFEST-PF Registry. *Circulation* 2023;148:35–46. <https://doi.org/10.1161/CIRCULATIONAHA.123.064959>.
- [31] Jiang S, Qian F, Ji S, Li L, Liu Q, Zhou S, et al. Pulsed Field Ablation for Atrial Fibrillation: Mechanisms, Advantages, and Limitations. *Rev Cardiovasc Med* 2024;25. <https://doi.org/10.31083/j.rcm2504138>.
- [32] Heijman J, Sutanto H, Crijns HJGM, Nattel S, Trayanova NA. Computational models of atrial fibrillation: achievements, challenges, and perspectives for improving clinical care. *Cardiovasc Res* 2021;117:1682–99. <https://doi.org/10.1093/cvr/cvab138>.
- [33] Pennes HH. *Analysis of Tissue and Arterial Blood Temperatures in the Resting Human Forearm*. *J Appl Physiol* 1948;1:93–122. <https://doi.org/10.1152/jappl.1948.1.2.93>.
- [34] Ziaei P, Moosavi H, Moradi A. Analysis of the dual phase lag bio-heat transfer equation with constant and time-dependent heat flux conditions on skin surface. *Thermal Science* 2016;20:1457–72. <https://doi.org/10.2298/TSCI140128057Z>.
- [35] Hristov J. Bio-Heat Models Revisited: Concepts, Derivations, Nondimensionalization and Fractionalization Approaches. *Front Phys* 2019;7. <https://doi.org/10.3389/fphys.2019.00189>.
- [36] Wang K, Tavakkoli F, Wang S, Vafai K. Analysis and analytical characterization of bioheat transfer during radiofrequency ablation. *J Biomech* 2015;48:930–40. <https://doi.org/10.1016/j.jbiomech.2015.02.023>.
- [37] Alba-Martinez J. Mathematical Models Based on Transfer Functions to Estimate Tissue Temperature During RF Cardiac Ablation in Real Time. *Open Biomed Eng J* 2012;6:16–22. <https://doi.org/10.2174/1874230001206010016>.
- [38] Singh S, Saccomandi P, Melnik R. Three-Phase-Lag Bio-Heat Transfer Model of Cardiac Ablation. *Fluids* 2022;7:180. <https://doi.org/10.3390/fluids7050180>.
- [39] Majchrzak E, Mochnacki B. Dual-phase lag equation. Stability conditions of a numerical algorithm based on the explicit scheme of the finite difference method. *Journal of Applied Mathematics and Computational Mechanics* 2016;15:89–96. <https://doi.org/10.17512/jamcm.2016.3.09>.

- [40] Singh S, Melnik R. Computational Modeling of Cardiac Ablation Incorporating Electrothermomechanical Interactions. *J Eng Sci Med Diagn Ther* 2020;3. <https://doi.org/10.1115/1.4048536>.
- [41] Krokidis M, Ahmed I. Overview of Thermal Ablation Devices: Radiofrequency Ablation. *Interventional Radiology Techniques in Ablation*, London: Springer London; 2013, p. 5–11. [https://doi.org/10.1007/978-0-85729-094-6\\_2](https://doi.org/10.1007/978-0-85729-094-6_2).
- [42] Dello Russo A, Compagnucci P, Anselmino M, Schillaci V, Campanelli F, Ascione MR, et al. Pulsed field vs very high-power short-duration radiofrequency ablation for atrial fibrillation: Results of a multicenter, real-world experience. *Heart Rhythm* 2024;21:1526–36. <https://doi.org/10.1016/j.hrthm.2024.05.042>.
- [43] Verma A, Neal R, Evans J, Castellvi Q, Vachani A, Deneke T, et al. Characteristics of pulsed electric field cardiac ablation porcine treatment zones with a focal catheter. *J Cardiovasc Electrophysiol* 2023;34:99–107. <https://doi.org/10.1111/jce.15734>.
- [44] Bathe K-J, Zhang H, Yan Y. The solution of Maxwell's equations in multiphysics. *Comput Struct* 2014;132:99–112. <https://doi.org/10.1016/j.compstruc.2013.09.006>.
- [45] Cobos Sanchez C, Garcia SG, Angulo LD, De Jong Van Coevorden CM, Rubio Bretones A. A DIVERGENCE-FREE BEM METHOD TO MODEL QUASI-STATIC CURRENTS: APPLICATION TO MRI COIL DESIGN. *Progress In Electromagnetics Research B* 2010;20:187–203. <https://doi.org/10.2528/PIERB10011504>.
- [46] Gonzalez-Suarez A, Berjano E. Comparative Analysis of Different Methods of Modeling the Thermal Effect of Circulating Blood Flow During RF Cardiac Ablation. *IEEE Trans Biomed Eng* 2016;63:250–9. <https://doi.org/10.1109/TBME.2015.2451178>.
- [47] Singh S, Melnik R. Fluid–Structure Interaction and Non-Fourier Effects in Coupled Electro-Thermo-Mechanical Models for Cardiac Ablation. *Fluids* 2021;6:294. <https://doi.org/10.3390/fluids6080294>.
- [48] Maxwell JC. VIII. A dynamical theory of the electromagnetic field. *Philos Trans R Soc Lond* 1865;155:459–512. <https://doi.org/10.1098/rstl.1865.0008>.
- [49] Doss JD. Calculation of electric fields in conductive media. *Med Phys* 1982;9:566–73. <https://doi.org/10.1118/1.595107>.
- [50] Ji X, Zhang H, Zang L, Yan S, Wu X. The Effect of Discharge Mode on the Distribution of Myocardial Pulsed Electric Field—A Simulation Study for Pulsed Field Ablation of Atrial Fibrillation. *J Cardiovasc Dev Dis* 2022;9:95. <https://doi.org/10.3390/jcdd9040095>.
- [51] Giannainas N, Sembakuttige LR, Das M. Radiofrequency Lesion Quality Markers: Current State of Knowledge. *Eur J Arrhythm Electrophysiol* 2022;8:2. <https://doi.org/10.17925/EJAE.2022.8.1.2>.



- [52] Chang IA. Considerations for Thermal Injury Analysis for RF Ablation Devices. *Open Biomed Eng J* 2010;4:3–12. <https://doi.org/10.2174/1874120701004020003>.
- [53] Nath S, Lynch C, Whayne JG, Haines DE. Cellular electrophysiological effects of hyperthermia on isolated guinea pig papillary muscle. Implications for catheter ablation. *Circulation* 1993;88:1826–31. <https://doi.org/10.1161/01.CIR.88.4.1826>.
- [54] Davalos R V., Mir LM, Rubinsky B. Tissue Ablation with Irreversible Electroporation. *Ann Biomed Eng* 2005;33:223–31. <https://doi.org/10.1007/s10439-005-8981-8>.
- [55] Tucci C, Trujillo M, Berjano E, Iasiello M, Andreozzi A, Vanoli GP. Pennes' bioheat equation vs. porous media approach in computer modeling of radiofrequency tumor ablation. *Sci Rep* 2021;11:5272. <https://doi.org/10.1038/s41598-021-84546-6>.
- [56] Tungjitkusolmun S, Vorperian VR, Bhavaraju N, Cao H, Tsai J-Z, Webster JG. Guidelines for predicting lesion size at common endocardial locations during radio-frequency ablation. *IEEE Trans Biomed Eng* 2001;48:194–201. <https://doi.org/10.1109/10.909640>.
- [57] HAINES DE, WATSON DD. Tissue Heating During Radiofrequency Catheter Ablation: A Thermodynamic Model and Observations in Isolated Perfused and Superfused Canine Right Ventricular Free Wall. *Pacing and Clinical Electrophysiology* 1989;12:962–76. <https://doi.org/10.1111/j.1540-8159.1989.tb05034.x>.
- [58] Sugrue A, Maor E, Del-Carpio Munoz F, Killu AM, Asirvatham SJ. Cardiac ablation with pulsed electric fields: principles and biophysics. *EP Europace* 2022;24:1213–22. <https://doi.org/10.1093/europace/euac033>.
- [59] Casciola M, Kaboudian A, Feaster TK, Narkar A, Blinova K. Pulsed electric field performance calculator tool based on an in vitro human cardiac model. *Front Physiol* 2024;15. <https://doi.org/10.3389/fphys.2024.1395923>.
- [60] Meckes D, Emami M, Fong I, Lau DH, Sanders P. Pulsed-field ablation: Computational modeling of electric fields for lesion depth analysis. *Heart Rhythm O2* 2022;3:433–40. <https://doi.org/10.1016/j.hroo.2022.05.009>.
- [61] Gómez-Barea M, García-Sánchez T, Ivorra A. A computational comparison of radiofrequency and pulsed field ablation in terms of lesion morphology in the cardiac chamber. *Sci Rep* 2022;12:16144. <https://doi.org/10.1038/s41598-022-20212-9>.
- [62] Simon "Richard, K. Mehta N, B. Shah K, Haines D, Linte" C. Toward a quasi-dynamic pulsed field electroporation numerical model for cardiac ablation: Predicting tissue conductance changes and ablation lesion patterns, 2022. <https://doi.org/10.22489/CinC.2022.233>.
- [63] Chang IA, Nguyen UD. Thermal modeling of lesion growth with radiofrequency ablation devices. *Biomed Eng Online* 2004;3:27. <https://doi.org/10.1186/1475-925X-3-27>.

- [64] Arrhenius S. Über die Reaktionsgeschwindigkeit bei der Inversion von Rohrzucker durch Säuren. *Zeitschrift Für Physikalische Chemie* 1889;4U:226–48. <https://doi.org/10.1515/zpch-1889-0416>.
- [65] Will M, Gerlach T, Saalfeld S, Gutberlet M, Dux D, Schröer S, et al. Temperature Simulation of an Ablation Needle for the Prediction of Tissue Necrosis during Liver Ablation. *J Clin Med* 2024;13:5853. <https://doi.org/10.3390/jcm13195853>.
- [66] Garcia PA, Davalos R V., Miklavcic D. A Numerical Investigation of the Electric and Thermal Cell Kill Distributions in Electroporation-Based Therapies in Tissue. *PLoS One* 2014;9:e103083. <https://doi.org/10.1371/journal.pone.0103083>.
- [67] Sapareto SA. Thermal isoeffect dose: Addressing the problem of thermotolerance. *International Journal of Hyperthermia* 1987;3:297–305. <https://doi.org/10.3109/02656738709140400>.
- [68] van Rhoon GC, Samaras T, Yarmolenko PS, Dewhurst MW, Neufeld E, Kuster N. CEM43°C thermal dose thresholds: a potential guide for magnetic resonance radiofrequency exposure levels? *Eur Radiol* 2013;23:2215–27. <https://doi.org/10.1007/s00330-013-2825-y>.
- [69] Sapareto SA, Dewey WC. Thermal dose determination in cancer therapy. *International Journal of Radiation Oncology\*Biophysics* 1984;10:787–800. [https://doi.org/10.1016/0360-3016\(84\)90379-1](https://doi.org/10.1016/0360-3016(84)90379-1).
- [70] Esmailie F, Francoeur M, Ameel T. Heat transfer analysis in an uncoiled model of the cochlea during magnetic cochlear implant surgery. *Int J Heat Mass Transf* 2020;154:119683. <https://doi.org/https://doi.org/10.1016/j.ijheatmasstransfer.2020.119683>.
- [71] Esmailie F, Francoeur M, Ameel T. Experimental Validation of a Three-Dimensional Heat Transfer Model Within the Scala Tympani With Application to Magnetic Cochlear Implant Surgery. *IEEE Trans Biomed Eng* 2021;68:2821–32. <https://doi.org/10.1109/TBME.2021.3055976>.
- [72] Esmailie F, Francoeur M, Ameel T. A three-dimensional thermal model of the human cochlea for magnetic cochlear implant surgery. *Int J Heat Mass Transf* 2021;178:121553. <https://doi.org/https://doi.org/10.1016/j.ijheatmasstransfer.2021.121553>.
- [73] Negussie AH, Morhard R, Rivera J, Delgado JF, Xu S, Wood BJ. Thermochromic phantoms and paint to characterize and model image-guided thermal ablation and ablation devices: a review. *Functional Composite Materials* 2024;5:1. <https://doi.org/10.1186/s42252-023-00050-2>.
- [74] Mouratidis PXE, Rivens I, Civale J, Symonds-Taylor R, ter Haar G. ‘Relationship between thermal dose and cell death for “rapid” ablative and “slow” hyperthermic heating.’ *International Journal of Hyperthermia* 2019;36:228–42. <https://doi.org/10.1080/02656736.2018.1558289>.
- [75] van Rhoon GC. Is CEM43 still a relevant thermal dose parameter for hyperthermia treatment monitoring? *International Journal of Hyperthermia* 2016;32:50–62. <https://doi.org/10.3109/02656736.2015.1114153>.

- [76] Baena-Montes JM, O'Halloran T, Clarke C, Donaghey K, Dunne E, O'Halloran M, et al. Electroporation Parameters for Human Cardiomyocyte Ablation In Vitro. *J Cardiovasc Dev Dis* 2022;9:240. <https://doi.org/10.3390/jcdd9080240>.
- [77] Dewey WC. Arrhenius relationships from the molecule and cell to the clinic. *International Journal of Hyperthermia* 1994;10:457–83. <https://doi.org/10.3109/02656739409009351>.
- [78] Edd JF, Davalos R V. Mathematical Modeling of Irreversible Electroporation for Treatment Planning. *Technol Cancer Res Treat* 2007;6:275–86. <https://doi.org/10.1177/153303460700600403>.
- [79] Peleg M. A model of microbial survival after exposure to pulsed electric fields. *J Sci Food Agric* 1995;67:93–9. <https://doi.org/10.1002/jsfa.2740670115>.
- [80] Golberg A, Rubinsky B. A statistical model for multidimensional irreversible electroporation cell death in tissue. *Biomed Eng Online* 2010;9:13. <https://doi.org/10.1186/1475-925X-9-13>.
- [81] Bianchi L, Cavarzan F, Ciampitti L, Cremonesi M, Grilli F, Saccomandi P. Thermophysical and mechanical properties of biological tissues as a function of temperature: a systematic literature review. *International Journal of Hyperthermia* 2022;39:297–340. <https://doi.org/10.1080/02656736.2022.2028908>.
- [82] Iacobellis G. Epicardial adipose tissue in contemporary cardiology. *Nat Rev Cardiol* 2022;19:593–606. <https://doi.org/10.1038/s41569-022-00679-9>.
- [83] Xie F, Zemlin CW. Effect of Twisted Fiber Anisotropy in Cardiac Tissue on Ablation with Pulsed Electric Fields. *PLoS One* 2016;11:e0152262. <https://doi.org/10.1371/journal.pone.0152262>.
- [84] Molinari L, Zaltieri M, Massaroni C, Filippi S, Gizzi A, Schena E. Multiscale and Multiphysics Modeling of Anisotropic Cardiac RFCA: Experimental-Based Model Calibration via Multi-Point Temperature Measurements. *Front Physiol* 2022;13. <https://doi.org/10.3389/fphys.2022.845896>.
- [85] TISSUE DB » IT'IS Foundation n.d. <https://itis.swiss/virtual-population/tissue-properties/database/> (accessed January 22, 2025).
- [86] Estevez-Laborí F, O'Brien B, González-Suárez A. Difference between endocardial and epicardial application of pulsed fields for targeting Epicardial Ganglia: An in-silico modelling study. *Comput Biol Med* 2024;174:108490. <https://doi.org/10.1016/J.COMPBIOMED.2024.108490>.
- [87] van Erp GCM, Hendriks P, Broersen A, Verhagen CAM, Gholamiankhah F, Dijkstra J, et al. Computational Modeling of Thermal Ablation Zones in the Liver: A Systematic Review. *Cancers (Basel)* 2023;15:5684. <https://doi.org/10.3390/cancers15235684>.
- [88] Andreozzi A, Iasiello M, Tucci C. An overview of mathematical models and modulated-heating protocols for thermal ablation, 2020, p. 489–541. <https://doi.org/10.1016/bs.aiht.2020.07.003>.
- [89] Zang L, Gu K, Ji X, Zhang H, Yan S, Wu X. Comparative Analysis of Temperature Rise between Convective Heat Transfer Method and Computational Fluid Dynamics Method in an Anatomy-

- Based Left Atrium Model during Pulsed Field Ablation: A Computational Study. *J Cardiovasc Dev Dis* 2023;10:56. <https://doi.org/10.3390/jcdd10020056>.
- [90] Razeghi O, Kapoor R, Alhusseini MI, Fazal M, Tang S, Roney CH, et al. Atrial fibrillation ablation outcome prediction with a machine learning fusion framework incorporating cardiac computed tomography. *J Cardiovasc Electrophysiol* 2023;34:1164–74. <https://doi.org/10.1111/jce.15890>.
- [91] Trayanova NA, Doshi AN, Prakosa A. How personalized heart modeling can help treatment of lethal arrhythmias: A focus on ventricular tachycardia ablation strategies in post-infarction patients. *WIREs Systems Biology and Medicine* 2020;12. <https://doi.org/10.1002/wsbm.1477>.
- [92] Hong Cao, Vorperian VR, Tungjitkusolmun S, Jan-Zern Tsai, Haemmerich D, Young Bin Choy, et al. Flow effect on lesion formation in RF cardiac catheter ablation. *IEEE Trans Biomed Eng* 2001;48:425–33. <https://doi.org/10.1109/10.915708>.
- [93] Gu K, Yan S, Wu X. Influence of pulsating intracardiac blood flow on radiofrequency catheter ablation outcomes in an anatomy-based atrium model. *International Journal of Hyperthermia* 2022;39:1064–77. <https://doi.org/10.1080/02656736.2022.2108149>.
- [94] Valvez S, Oliveira-Santos M, Piedade AP, Gonçalves L, Amaro AM. Computational Flow Dynamic Analysis in Left Atrial Appendage Thrombus Formation Risk: A Review. *Applied Sciences* 2023;13:8201. <https://doi.org/10.3390/app13148201>.
- [95] Radmilović-Radjenović M, Sabo M, Prnova M, Šoltes L, Radjenović B. Finite Element Analysis of the Microwave Ablation Method for Enhanced Lung Cancer Treatment. *Cancers (Basel)* 2021;13:3500. <https://doi.org/10.3390/cancers13143500>.
- [96] González-Suárez A, Pérez JJ, Irastorza RM, D'Avila A, Berjano E. Computer modeling of radiofrequency cardiac ablation: 30 years of bioengineering research. *Comput Methods Programs Biomed* 2022;214:106546. <https://doi.org/10.1016/j.cmpb.2021.106546>.
- [97] Li X, Yamaji A. A numerical study of isotropic and anisotropic ablation in MCCI by MPS method. *Progress in Nuclear Energy* 2016;90:46–57. <https://doi.org/10.1016/j.pnucene.2016.03.001>.
- [98] Marla D, Bhandarkar U V., Joshi SS. Transient Analysis of Laser Ablation Process With Plasma Shielding: One-Dimensional Model Using Finite Volume Method. *J Micro Nanomanuf* 2013;1. <https://doi.org/10.1115/1.4023287>.
- [99] Amar AJ, Blackwell BF, Edwards JR. One-Dimensional Ablation Using a Full Newton's Method and Finite Control Volume Procedure. *J Thermophys Heat Trans* 2008;22:71–82. <https://doi.org/10.2514/1.29610>.
- [100] Boon JP. The Lattice Boltzmann Equation for Fluid Dynamics and Beyond. *European Journal of Mechanics - B/Fluids* 2003;22:101. [https://doi.org/10.1016/S0997-7546\(02\)00005-5](https://doi.org/10.1016/S0997-7546(02)00005-5).

- [101] Rapaka S, Mansi T, Georgescu B, Pop M, Wright GA, Kamen A, et al. LBM-EP: Lattice-Boltzmann Method for Fast Cardiac Electrophysiology Simulation from 3D Images, 2012, p. 33–40. [https://doi.org/10.1007/978-3-642-33418-4\\_5](https://doi.org/10.1007/978-3-642-33418-4_5).
- [102] Kawamura I, Reddy VY, Wang BJ, Dukkipati SR, Chaudhry HW, Santos-Gallego CG, et al. Pulsed Field Ablation of the Porcine Ventricle Using a Focal Lattice-Tip Catheter. *Circ Arrhythm Electrophysiol* 2022;15. <https://doi.org/10.1161/CIRCEP.122.011120>.
- [103] Osman AFI, Maalej NM, Jayesh K. Prediction of the individual multileaf collimator positional deviations during dynamic IMRT delivery *priori* with artificial neural network. *Med Phys* 2020;47:1421–30. <https://doi.org/10.1002/mp.14014>.
- [104] Park J-W, Kwon O-S, Shim J, Hwang I, Kim YG, Yu HT, et al. Machine Learning-Predicted Progression to Permanent Atrial Fibrillation After Catheter Ablation. *Front Cardiovasc Med* 2022;9. <https://doi.org/10.3389/fcvm.2022.813914>.
- [105] Negro R, Rucco M, Creanza A, Mormile A, Limone PP, Garberoglio R, et al. Machine Learning Prediction of Radiofrequency Thermal Ablation Efficacy: A New Option to Optimize Thyroid Nodule Selection. *Eur Thyroid J* 2020;9:205–12. <https://doi.org/10.1159/000504882>.
- [106] Moreira P, Tuncali K, Tempany C, Tokuda J. AI-Based Isotherm Prediction for Focal Cryoablation of Prostate Cancer. *Acad Radiol* 2023;30:S14–20. <https://doi.org/10.1016/j.acra.2023.04.016>.
- [107] Tang S, Razeghi O, Kapoor R, Alhuseini MI, Fazal M, Rogers AJ, et al. Machine Learning–Enabled Multimodal Fusion of Intra-Atrial and Body Surface Signals in Prediction of Atrial Fibrillation Ablation Outcomes. *Circ Arrhythm Electrophysiol* 2022;15. <https://doi.org/10.1161/CIRCEP.122.010850>.
- [108] Ashour AS, Guo Y, Mohamed WS. COMSOL Multiphysics software for ablation system simulation. *Thermal Ablation Therapy*, Elsevier; 2021, p. 221–89. <https://doi.org/10.1016/B978-0-12-819544-4.00007-1>.
- [109] Pérez JJ, González-Suárez A. How intramyocardial fat can alter the electric field distribution during Pulsed Field Ablation (PFA): Qualitative findings from computer modeling. *PLoS One* 2023;18:e0287614. <https://doi.org/10.1371/journal.pone.0287614>.
- [110] Kanth P V, Murthy V B, Mohan R C. Simulation of Thermal Ablation Process using ANSYS Software. *International Journal of Innovative Technology and Exploring Engineering* 2019;9:4941–2. <https://doi.org/10.35940/ijitee.A8119.119119>.
- [111] Pérez JJ, González-Suárez A, Berjano E. Numerical analysis of thermal impact of intramyocardial capillary blood flow during radiofrequency cardiac ablation. *International Journal of Hyperthermia* 2018;34:243–9. <https://doi.org/10.1080/02656736.2017.1336258>.
- [112] Jankelson L, Dai M, Bernstein S, Park D, Holmes D, Aizer A, et al. Quantitative analysis of ablation technique predicts arrhythmia recurrence following atrial fibrillation ablation. *Am Heart J* 2020;220:176–83. <https://doi.org/10.1016/j.ahj.2019.11.011>.

- [113] Sulkin MS, Laughner JI, Rogge M, Philpott JM, Efimov IR. Dual cryo-radiofrequency ablation enhances lesion depth in beating human left ventricular preparations 2018. <https://doi.org/10.1101/469882>.
- [114] Seno H, Yamazaki M, Shibata N, Sakuma I, Tomii N. In-Silico Deep Reinforcement Learning for Effective Cardiac Ablation Strategy. *J Med Biol Eng* 2021;41:953–65. <https://doi.org/10.1007/s40846-021-00664-6>.
- [115] Hirota N, Suzuki S, Arita T, Yagi N, Otsuka T, Yamashita T. Prediction of recurrence after catheter ablation for atrial fibrillation using left atrial morphology on preprocedural computed tomography: application of radiomics. *Eur Heart J* 2022;43. <https://doi.org/10.1093/eurheartj/ehac544.597>.
- [116] Wang H, Barbhaiya CR, Yuan Y, Barbee D, Chen T, Axel L, et al. A Tool to Integrate Electrophysiological Mapping for Cardiac Radioablation of Ventricular Tachycardia. *Adv Radiat Oncol* 2023;8:101272. <https://doi.org/10.1016/j.adro.2023.101272>.
- [117] Murray-Smith DJ. The Use of Experimental Data in Simulation Model Validation, 2019, p. 357–82. [https://doi.org/10.1007/978-3-319-70766-2\\_15](https://doi.org/10.1007/978-3-319-70766-2_15).
- [118] Prakosa A, Arevalo HJ, Deng D, Boyle PM, Nikolov PP, Ashikaga H, et al. Personalized virtual-heart technology for guiding the ablation of infarct-related ventricular tachycardia. *Nat Biomed Eng* 2018;2:732–40. <https://doi.org/10.1038/s41551-018-0282-2>.
- [119] Rossmann C, Motamarry A, Panescu D, Haemmerich D. Computer simulations of an irrigated radiofrequency cardiac ablation catheter and experimental validation by infrared imaging. *International Journal of Hyperthermia* 2021;38:1149–63. <https://doi.org/10.1080/02656736.2021.1961027>.
- [120] González-Suárez A, Berjano E, Guerra JM, Gerardo-Giorda L. Computational Modeling of Open-Irrigated Electrodes for Radiofrequency Cardiac Ablation Including Blood Motion-Saline Flow Interaction. *PLoS One* 2016;11:e0150356. <https://doi.org/10.1371/journal.pone.0150356>.
- [121] Petras A, Leoni M, Guerra JM, Jansson J, Gerardo-Giorda L. A computational model of open-irrigated radiofrequency catheter ablation accounting for mechanical properties of the cardiac tissue. *Int J Numer Method Biomed Eng* 2019;35. <https://doi.org/10.1002/cnm.3232>.
- [122] D’Silva A, Wright M. Advances in Imaging for Atrial Fibrillation Ablation. *Radiol Res Pract* 2011;2011:1–10. <https://doi.org/10.1155/2011/714864>.
- [123] Calvert P, Mills MT, Xydis P, Essa H, Ding WY, Koniari I, et al. Cost, efficiency, and outcomes of pulsed field ablation vs thermal ablation for atrial fibrillation: A real-world study. *Heart Rhythm* 2024;21:1537–44. <https://doi.org/10.1016/j.hrthm.2024.05.032>.
- [124] Tzeis S, Gerstenfeld EP, Kalman J, Saad EB, Sepeshri Shamloo A, Andrade JG, et al. 2024 European Heart Rhythm Association/Heart Rhythm Society/Asia Pacific Heart Rhythm Society/Latin American Heart Rhythm Society expert consensus statement on catheter and surgical ablation of atrial fibrillation. *Europace* 2024;26. <https://doi.org/10.1093/europace/ueae043>.

- [125] Reynolds MR, Zimetbaum P, Josephson ME, Ellis E, Danilov T, Cohen DJ. Cost-Effectiveness of Radiofrequency Catheter Ablation Compared With Antiarrhythmic Drug Therapy for Paroxysmal Atrial Fibrillation. *Circ Arrhythm Electrophysiol* 2009;2:362–9. <https://doi.org/10.1161/CIRCEP.108.837294>.
- [126] Guo F, Wang J, Zhou L, Wang Y, Jiang H, Yu L. Advances in the Application of Pulsed Field Ablation for Arrhythmia Treatment. *Cardiovasc Innov Appl* 2023;8. <https://doi.org/10.15212/CVIA.2023.0019>.
- [127] Wittkamp FHM, Wever EFD, Derksen R, Wilde AAM, Ramanna H, Hauer RNW, et al. LocaLisa: new technique for real-time 3-dimensional localization of regular intracardiac electrodes. *Circulation* 1999;99:1312–7. <https://doi.org/10.1161/01.CIR.99.10.1312>.
- [128] Lim B, Kim J, Hwang M, Song J-S, Lee JK, Yu H-T, et al. In situ procedure for high-efficiency computational modeling of atrial fibrillation reflecting personal anatomy, fiber orientation, fibrosis, and electrophysiology. *Sci Rep* 2020;10:2417. <https://doi.org/10.1038/s41598-020-59372-x>.
- [129] Alessandrini M, Valinoti M, Unger L, Oesterlein T, Dössel O, Corsi C, et al. A Computational Framework to Benchmark Basket Catheter Guided Ablation in Atrial Fibrillation. *Front Physiol* 2018;9. <https://doi.org/10.3389/fphys.2018.01251>.
- [130] Linte CA, Camp JJ, Rettmann ME, Haemmerich D, Aktas MK, Huang DT, et al. Lesion modeling, characterization, and visualization for image-guided cardiac ablation therapy monitoring. *Journal of Medical Imaging* 2018;5:1. <https://doi.org/10.1117/1.JMI.5.2.021218>.
- [131] Mesquita J, Ferreira AM, Cavaco D, Moscoso Costa F, Carmo P, Marques H, et al. Development and validation of a risk score for predicting atrial fibrillation recurrence after a first catheter ablation procedure – ATLAS score. *EP Europace* 2018;20:f428–35. <https://doi.org/10.1093/europace/eux265>.
- [132] Belalcazar A. Safety and efficacy aspects of pulsed field ablation catheters as a function of electrode proximity to blood and energy delivery method. *Heart Rhythm O2* 2021;2:560–9. <https://doi.org/10.1016/j.hroo.2021.10.004>.
- [133] Rivera SI, Bernal CP, Martínez-Peláez R, Robledo-Nolasco R, De León-Larios G, Félix VG, et al. Computer Simulation of Catheter Cryoablation for Pulmonary Vein Isolation. *Healthcare* 2024;12:1508. <https://doi.org/10.3390/healthcare12151508>.
- [134] Patel T, Li C, Raissi F, Kassab GS, Gao T, Lee LC. Coupled thermal-hemodynamics computational modeling of cryoballoon ablation for pulmonary vein isolation. *Comput Biol Med* 2023;157:106766. <https://doi.org/10.1016/j.compbiomed.2023.106766>.
- [135] Baek Y-S, Kwon O-S, Lim B, Yang S-Y, Park J-W, Yu HT, et al. Clinical Outcomes of Computational Virtual Mapping-Guided Catheter Ablation in Patients With Persistent Atrial Fibrillation: A Multicenter Prospective Randomized Clinical Trial. *Front Cardiovasc Med* 2021;8. <https://doi.org/10.3389/fcvm.2021.772665>.

- [136] Li C, Lim B, Hwang M, Song J-S, Lee Y-S, Joung B, et al. The Spatiotemporal Stability of Dominant Frequency Sites in In-Silico Modeling of 3-Dimensional Left Atrial Mapping of Atrial Fibrillation. *PLoS One* 2016;11:e0160017. <https://doi.org/10.1371/journal.pone.0160017>.
- [137] Zhao J, Hansen BJ, Wang Y, Csepe TA, Sul L V., Tang A, et al. Three-dimensional Integrated Functional, Structural, and Computational Mapping to Define the Structural “Fingerprints” of Heart-Specific Atrial Fibrillation Drivers in Human Heart Ex Vivo. *J Am Heart Assoc* 2017;6. <https://doi.org/10.1161/JAHA.117.005922>.
- [138] Furui K, Morishima I, Morita Y, Kanzaki Y, Takagi K, Yoshida R, et al. Predicting long-term freedom from atrial fibrillation after catheter ablation by a machine learning algorithm: Validation of the CAAP-AF score. *J Arrhythm* 2020;36:297–303. <https://doi.org/10.1002/joa3.12303>.
- [139] Jolaei M, Hooshiar A, Dargahi J, Packirisamy M. Toward Task Autonomy in Robotic Cardiac Ablation: Learning-Based Kinematic Control of Soft Tendon-Driven Catheters. *Soft Robot* 2021;8:340–51. <https://doi.org/10.1089/soro.2020.0006>.
- [140] Budzianowski J, Hiczekiewicz J, Burchardt P, Pieszko K, Rzeźniczak J, Budzianowski P, et al. Predictors of atrial fibrillation early recurrence following cryoballoon ablation of pulmonary veins using statistical assessment and machine learning algorithms. *Heart Vessels* 2019;34:352–9. <https://doi.org/10.1007/s00380-018-1244-z>.
- [141] Singh S, Melnik R. Thermal ablation of biological tissues in disease treatment: A review of computational models and future directions. *Electromagn Biol Med* 2020;39:49–88. <https://doi.org/10.1080/15368378.2020.1741383>.
- [142] Zager Y, Kain D, Landa N, Leor J, Maor E. Optimization of Irreversible Electroporation Protocols for In-vivo Myocardial Decellularization. *PLoS One* 2016;11:e0165475. <https://doi.org/10.1371/journal.pone.0165475>.
- [143] Lozoya RC, Berte B, Cochet H, Jais P, Ayache N, Sermesant M. Model-Based Feature Augmentation for Cardiac Ablation Target Learning From Images. *IEEE Trans Biomed Eng* 2019;66:30–40. <https://doi.org/10.1109/TBME.2018.2818300>.